RSC Advances

REVIEW

View Article Online
View Journal | View Issue

Cite this: *RSC Adv.*, 2018, **8**, 4671

The influence of *Bacillus subtilis* on tin-coated copper in an aqueous environment

Ruilin Xiong,†[a] Kui Xiao, †*[a] Pan Yi,[a] Yuting Hu,[a] Chaofang Dong, [a] Junsheng Wu[a] and Xiaogang Li[ab]

Received 17th July 2017
Accepted 10th January 2018

DOI: 10.1039/c7ra07864a

rsc.li/rsc-advances

The influence of Bacillus subtilis (BS) on tin-coated copper in an aqueous environment was investigated by exposing the sample to a culture medium inoculated with BS. Scanning electron microscopy, electrochemical measurements and chemical analyses were performed to study the corrosion mechanism. The experimental results show that BS can adhere and gather on the surface of the sample, resulting in oxygen consumption at the place where the bacteria are densely attached. Increases in the R_{ct} values after the initial immersion showed that corrosion was inhibited, while decreases in the R_{ct} values after the later immersion showed that corrosion was accelerated. Our results suggest that differences in oxygen concentration due to activity of BS are the main reason for corrosion of tin-coated copper.

1. Introduction

Copper is a common material widely used in residential, commercial and industrial plumbing devices due to its useful properties.[1] However, copper suffers from corrosion damage due to chlorides, sulphides, particulates and microorganisms in its environment.[2–5] Coating copper with another kind of metal can improve its conductivity and welding properties. Coating copper with tin by using hot air solder levelling, as was performed in this study, is widely applied in the fabrication of commercial electronic devices because of the low cost, good solderability, and reliability of tin.[6]

Although copper has some antimicrobial properties, microbial corrosion of copper still occurs.[7–9] *Bacillus subtilis* (BS) has been studied in recent years because it has been isolated from many damaged industrial devices.[10–14] Yang *et al.*[15–17] found that microorganisms can attach to and destroy communication equipment and circuit boards, and BS is the predominant strain found on corroded surfaces. Currently, microbial corrosion due to BS on steel and alloys is being studied.[18–21] Zuo[22] studied the corrosion behaviour of Al 2024 exposed to artificial seawater (AS) in the presence of a protective biofilm of BS WB600 and found that the corrosion protection of Al 2024 in AS occurs only in the presence of a live biofilm. This is because the negatively-charged bacteria cause the biofilm to repel chloride ions, thereby increasing the E_{pit}. Qing[23] demonstrated that the corrosion of cold rolled steel (CRS) is accelerated by the lactic acid produced by BS in the initial corrosion of CRS in AS. The protection effect of the biofilm predominates later in the process because the biofilm can consume oxygen and produce a metabolic product that acts as a corrosion inhibitor for the CRS. Jayaraman *et al.*[24,25] studied the corrosion inhibition of carbon steel coupons immersed in a complex liquid medium (LB broth) and a synthetic seawater (VNSS) medium with seven diverse bacterial genera through oxygen depletion. It is possible that the different culture media led to different bacterial distributions and different corrosion mechanisms in Javed's studies.[26]

The aim of this study was to try to investigate the influence of BS on the corrosion behaviour of copper with a tin coating. BS is the predominant strain separated from the surface of tin-coated copper exposed to an atmospheric environment in Xishuangbanna. To clearly illustrate the effects of the biofilm on the corrosion behaviour of the tin-coated copper, a sodium nitrate culture medium was used to assess the corrosion effects of chloride. Tryptone in the LB culture medium was dissolved into ammonia during the bacterial metabolism process, and the alkaline environment protected the sample from the acidic environment. X-ray photoelectron spectroscopy (XPS) and energy-dispersive spectrometry (EDS) in this experiment were used to analyse the corrosion products of tin and copper in the presence of BS. Scanning environmental microscopy (ESEM) and fluorescence microscopy (FM) were used to characterise the corrosion morphology. Electrochemical impendence spectroscopy (EIS) was performed to evaluate the effects of BS on the corrosion behaviour of the sample.

2. Experimental methods

2.1 Materials

The sample was finished by coating the surface with lead-free spray tin and levelling it with heated and compressed air. The

[a]*Corrosion and Protection Center, University of Science and Technology Beijing, Beijing, 100083, P. R. China*

[b]*Ningbo Institute of Material Technology & Engineering, Chinese Academy of Sciences, Ningbo, 315201, P. R. China*

† These authors contributed equally to this work.

cross-sectional view of the sample is presented in Fig. 1. The tin layer was 1.4 μm thick. Each specimen was sterilised in a 75% ethanol solution for 2 h and then exposed to UV light for 30 min prior to use.

The culture medium consisted of the following components: 10 g L^{-1} of tryptone, 5 g L^{-1} of yeast extract, and 10 g L^{-1} of $NaNO_3$. The solution was sterilized by autoclaving it for 20 min at 121 °C at 100 kPa.

BS was isolated and purified from the corrosion area of the tin-coated copper, which was exposed to a semi-enclosed atmospheric environment in Xishuangbanna for a month. The BS was inoculated in an Erlenmeyer flask with 50 mL of sterilised culture medium and incubated at 37 °C. The initial cell concentration of the BS was adjusted to approximately 10^6 cells per mL.

2.2 Elemental analysis (XPS)

For the elemental analysis, the specimens were quickly removed from the culture media after immersion for 14 days and gently rinsed three times with sterilised water. After blow-drying with pure nitrogen, the specimens were stored in an airtight vacuum desiccator prior to use.

Scanning electron microscopy (SEM, FEI Quanta 250) was used to observe the morphology of the surface corrosion, and energy-dispersive spectrometry (EDS) analysis was used to determine the composition of the corrosion products. Elemental mapping of the enlarged map was used to obtain the distribution of elements on the surface. X-ray photoelectron spectroscopy (XPS) measurements were obtained on an X-ray photoelectron spectroscope (Thermo escalab 250Xi).

2.3 Fluorescence microscopy (FM)

After exposure to the culture medium inoculated with BS and without renewing the media for 7 and 14 days in the 37 °C incubator, the sample was taken out and washed twice with sterile phosphate buffered saline (PBS) solution to remove the dead and loosely attached bacteria. The samples were then stained with a colouring agent called Live-Dye for 15 min. 3 μL of green fluorescent dye (SYTO-9), which easily stains live cells, and 3 μL of iodinated pyridine (PI), which stains dead cells, were mixed into a mixture when staining. Images of the specimens with immobilised bacterial cells were taken at 100× magnification using an inverted fluorescence microscope (DSY5000×) equipped for epifluorescence with a mercury lamp. The live cells exhibited green fluorescence and the dead cells exhibited red fluorescence.

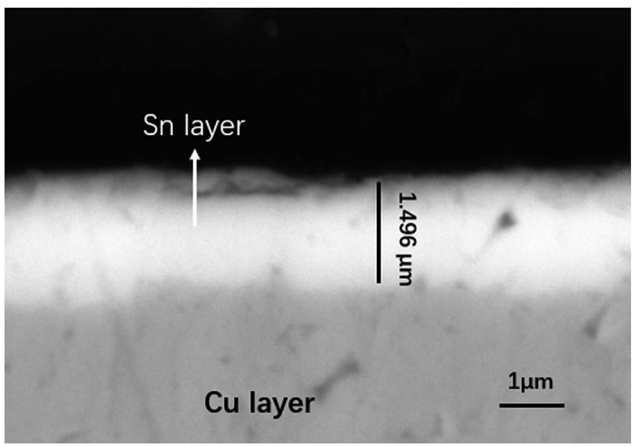

Fig. 1 Cross-sectional view of the sample.

2.4 Growth curve measurement

Growth curve experiments were performed to determine the growth tendency of BS in culture medium. BS was inoculated in a 50 mL Erlenmeyer flask with sterile culture medium and was active cultured for 10 h. Three 100 μL samples of culture medium were sucked inside a 1.5 mL EP tube. 200 mg L^{-1} of Cu^{2+} was added to one sample, and 200 mg L^{-1} of Sn^{4+} was added to another sample. 2 μL of active cultured BS medium was added to the 1.5 mL EP tube. Next, the 1.5 EP tube was placed into an automatic growth curve analyser (Bioscreen C). The automatic growth curve analyser measured the turbidity of the sample and automatically detected the optical density (OD) of the medium inoculated with BS at 30 °C.

2.5 Surface morphology

Each sample was immersed in media, both with and without BS inoculation, in a 37 °C incubator. After immersion for 7 and 14 days, the samples were taken out and washed with PBS solution to remove the floating bacteria. The samples were then immersed in 2.5% glutaraldehyde for 10 hours and dehydrated using a series of aqueous ethanol solutions (15%, 30%, 50%, 70%, 95% and 100%) for 15 min each. They were then coated with gold, and observed using field emission environment scanning electron microscopy (QUANTA FEG 250, USA).

2.6 Electrochemical measurements

A three-electrode system including a working electrode, an auxiliary electrode and a reference electrode was used for the electrochemical measurements. The working electrodes were made of tin-coated copper, connected with copper wire and mounted in silica gel with an exposed area of 1.2 cm^2. They were then washed twice with sterile water, sterilised with 75% ethanol solution for 2 h and finally exposed to UV light for 30 min to further sterilise them. The auxiliary electrode comprised platinum foil, and the reference electrode was a saturated calomel electrode (SCE) with a lugging capillary positioned close to the working electrode surface in order to minimise ohmic potential drop.

EIS measurements were conducted at the end of the open circuit potential (OCP) with a frequency range of 0.01–10^5 Hz using a PAR2273 advanced electrochemical system from Princeton Applied Research. All experiments were performed in the culture medium in an incubator. The experimental temperature was kept at 37 °C throughout the entire process using a thermostatically controlled water tank. Each experiment was repeated at least three times to ensure reproducibility.

3. Results and discussion

3.1 Surface chemical analysis

Fig. 2 shows the wide-scan XPS results for the sample surfaces after immersion in culture media with BS for 14 days. The tin peak of the sample surface after immersion in culture media with BS for 14 days appeared as shown in Fig. 2a, but the copper peak did not. This indicates that the copper substrate of the sample did not corrode after immersion in sterilised culture media, but the copper substrate of the sample did corrode after immersion in culture media with BS. Fig. 2b shows that the corrosion product under the sterile aqueous environment was SnO_2. The corrosion products under the aqueous environment with BS were SnO_2 and copper oxide. Cu(I) existed mainly in the form of Cu_2O, while Cu(II) was mainly in the form of CuO. The presence of Cu_2O indicates that the copper was not completely oxidised, which can be seen in Fig. 2d. The XPS results demonstrate that the tin-coated copper under the aqueous environment with BS was damaged more severely.

Fig. 3 shows the SEM image of the sample surfaces after immersion in culture media with BS for 14 days. The RACE (relative atomic concentrations of elements) values of the surfaces are summarised in Table 1. Fig. 4 shows that the surface contained the elements P, C, N, Sn, O, Cu, and Na. Phosphorus may have originated from the metabolites of the bacteria. Carbon and nitrogen may have originated partly from the metabolites and partly from the culture medium.

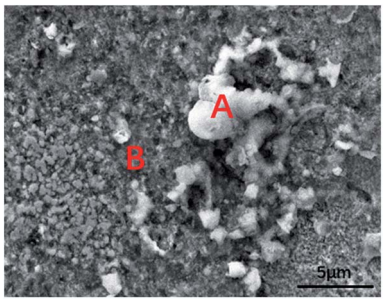

Fig. 3 SEM image of the surface of the sample immersed for 14 days.

Table 1 EDS of tin-coated copper after immersion for 14 days as shown in Fig. 5 (at%)

Element	C	Cu	Na	O	P	Sn
A	23.75	6.28	5.86	43.00	03.20	17.91
B	29.98	27.96	0.99	14.69	0.26	26.11

The amount of carbon and phosphorus found in the corrosion products on the sample under the sterile aqueous environment was minimal, but the amount of carbon and phosphorus found in those under the aqueous environment with BS was large. This implies that the corrosion products from the sample immersed in BS mainly originated from the

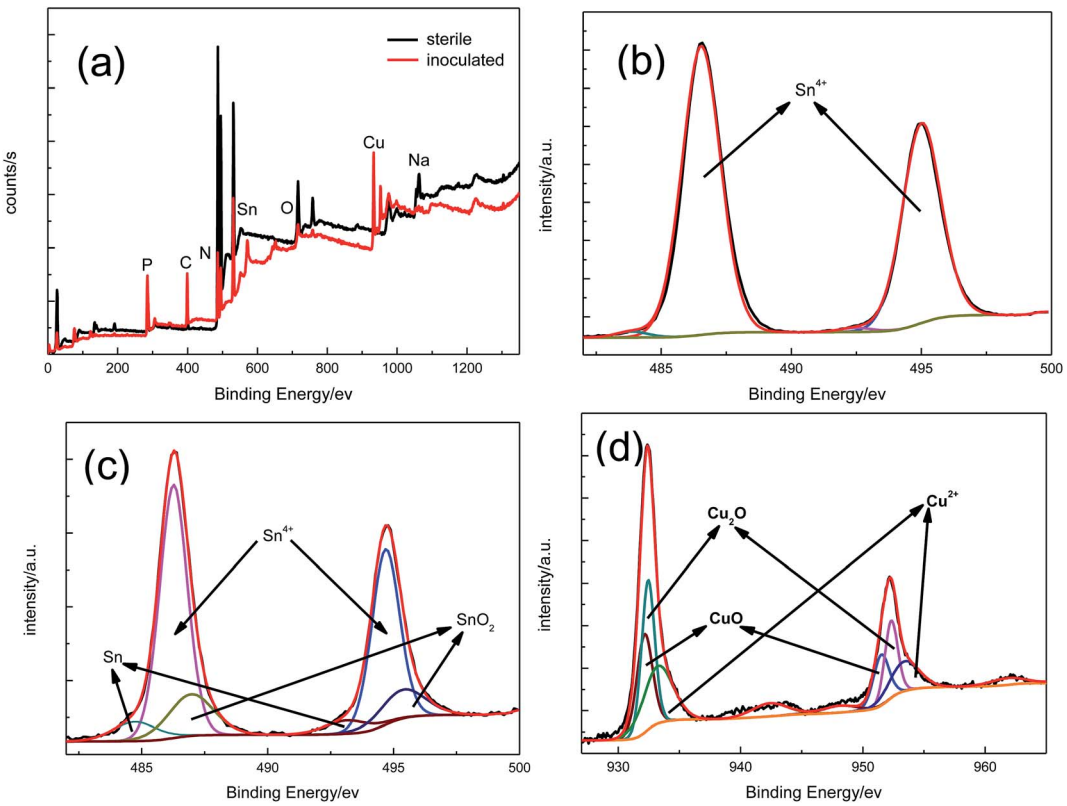

Fig. 2 Wide-scan XPS spectra (a) and high-resolution XPS spectra observed for the surface of the tin-coated copper exposed to sterile (b) and *Bacillus subtilis* (c and d) media for 14 days.

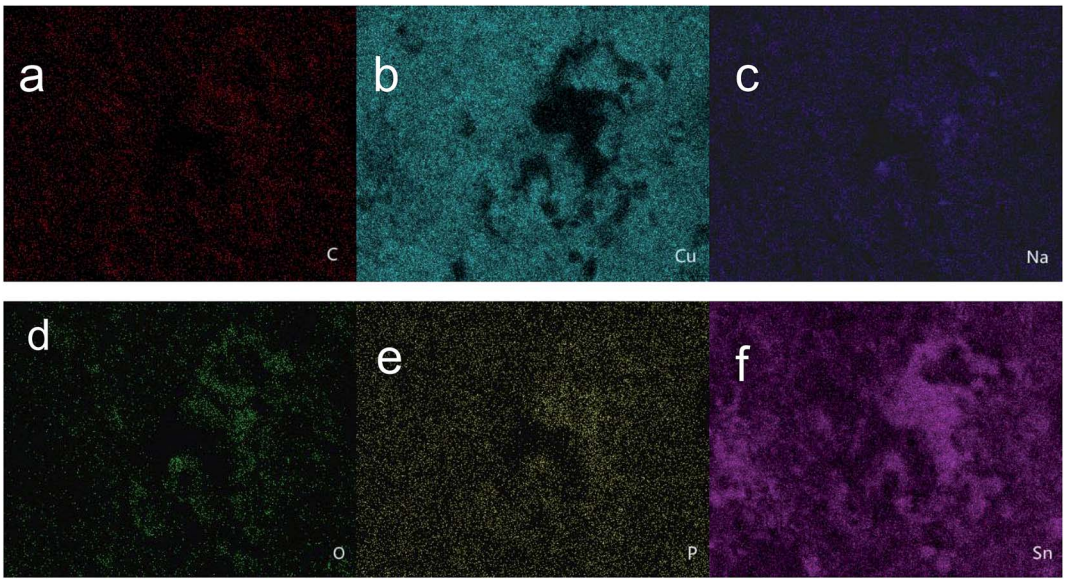

Fig. 4 EDS mapping results of (a) C, (b) Cu, (c) Na, (d) O, (e) P, and (f) Sn (at%).

metabolites of the bacteria. Sodium mainly originated from the sodium salt in the culture medium. The elemental mapping results in Fig. 4a and e show that the metabolites were widely distributed on the surface of the sample. Sn and Cu were the base elements of the sample. The amounts of oxygen and tin in A were much higher than those of the other elements, which indicates that more water-insoluble tin oxide was generated.

3.2 Bacterial colonisation study with FM

Fig. 5 shows the fluorescence images of the tin-coated copper under the aqueous environment with BS for 7 days (a and b) and 14 days (c and d). From the image of the sample immersed for 7 days, it can be seen that only a few live bacteria along with some dead bacteria were attached to the material surface. The surface of the tin-coated copper was covered with small pits. From the surface image of the tin-coated copper immersed for 14 days, it can be seen that more bacteria were attached to the sample. BS covered the surface in layers and gradually aggregated into a thick biofilm within an extracellular matrix containing polysaccharides, proteins and nucleic acids. The pitting gradually expanded, and the surface of the sample showed large corrosion product particles with many live and some dead bacteria accumulated on the material surface.

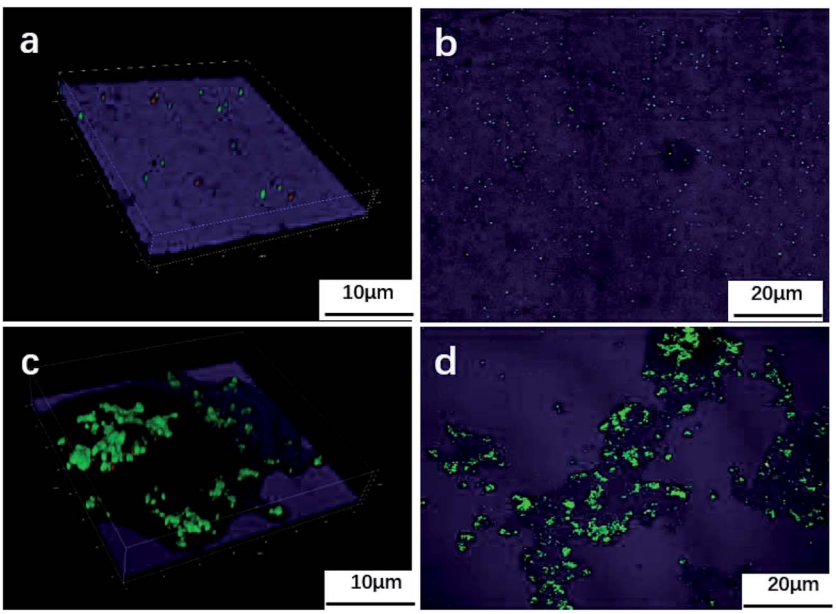

Fig. 5 Fluorescence images of bacterial colonies on the sample in the culture media after 7 days (a and b) and 14 days (c and d).

3.3 Surface morphology

Fig. 6 shows the SEM images of the sample after immersion in sterile culture medium for 14 days and with BS for 7 and 14 days. No significant cracks or corrosion pits appeared on the surface of the sample under the aqueous environment with BS for 7 days. Some bacteria surrounded by a small porous agglomeration of corrosion products were attached on the surface of the sample. There were also some small pits on the surface of the sample. More and more bacteria and corrosion products attached themselves onto the sample under the aqueous environment with BS for 14 days, as shown in Fig. 6e and f. When the corrosion products were removed, there were some larger holes on the sample under the aqueous environment with BS for 14 days, as shown in Fig. 6h. A more serious corrosion phenomenon was observed on the sample under the aqueous environment with BS (Fig. 6h) compared to the sterile aqueous environment (Fig. 6g).

3.4 EIS results

EIS is frequently used as a non-destructive technique to study electrochemical reactions at metal/biofilm interfaces, as well as

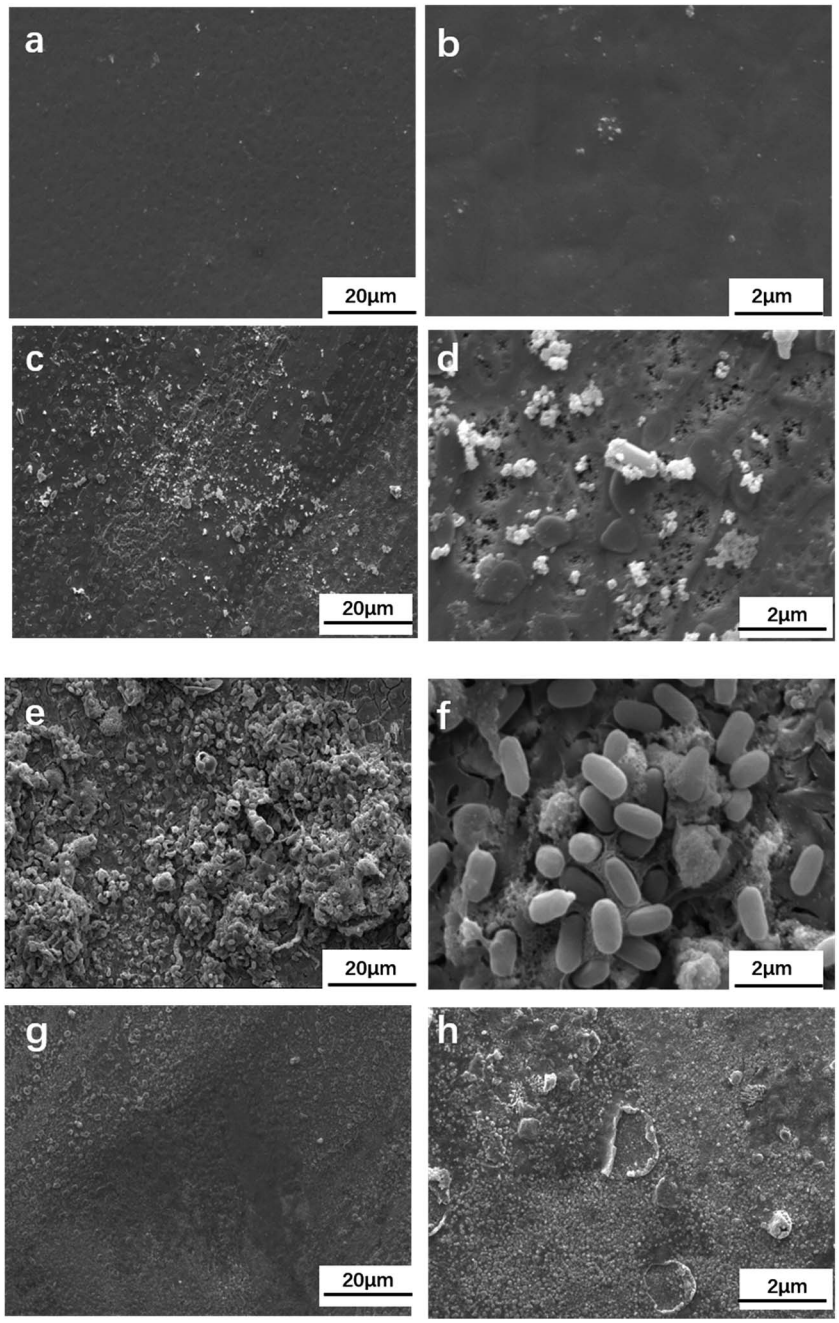

Fig. 6 SEM images of the tin-coated copper exposed to sterile culture medium for 14 days (a and b) and culture medium with BS for 14 days (c and d) and 7 days (e and f). SEM images of the sample exposed to the sterile culture medium with removal of the corrosion products and culture medium with BS for 14 days (g and h).

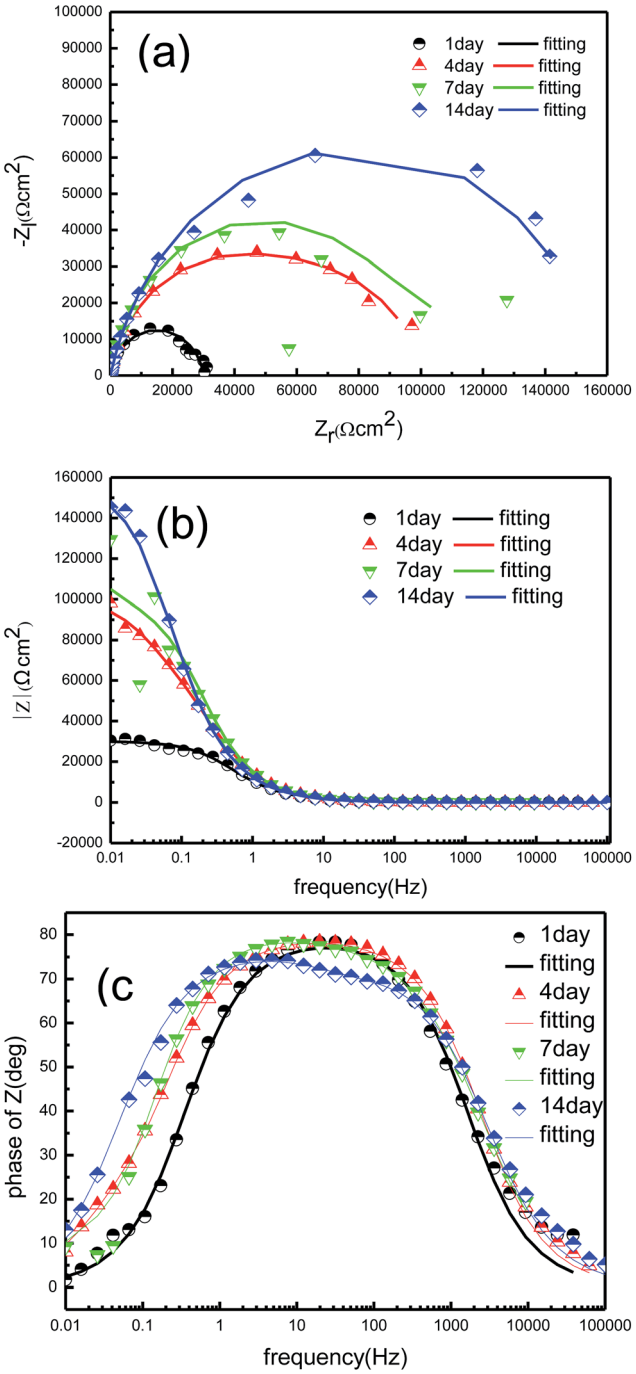

Fig. 7 EIS of the tin-coated copper immersed for different times in the sterile culture medium at 37 °C: (a) Nyquist plot, (b) Bode modulus diagram and (c) Bode phase angle diagram.

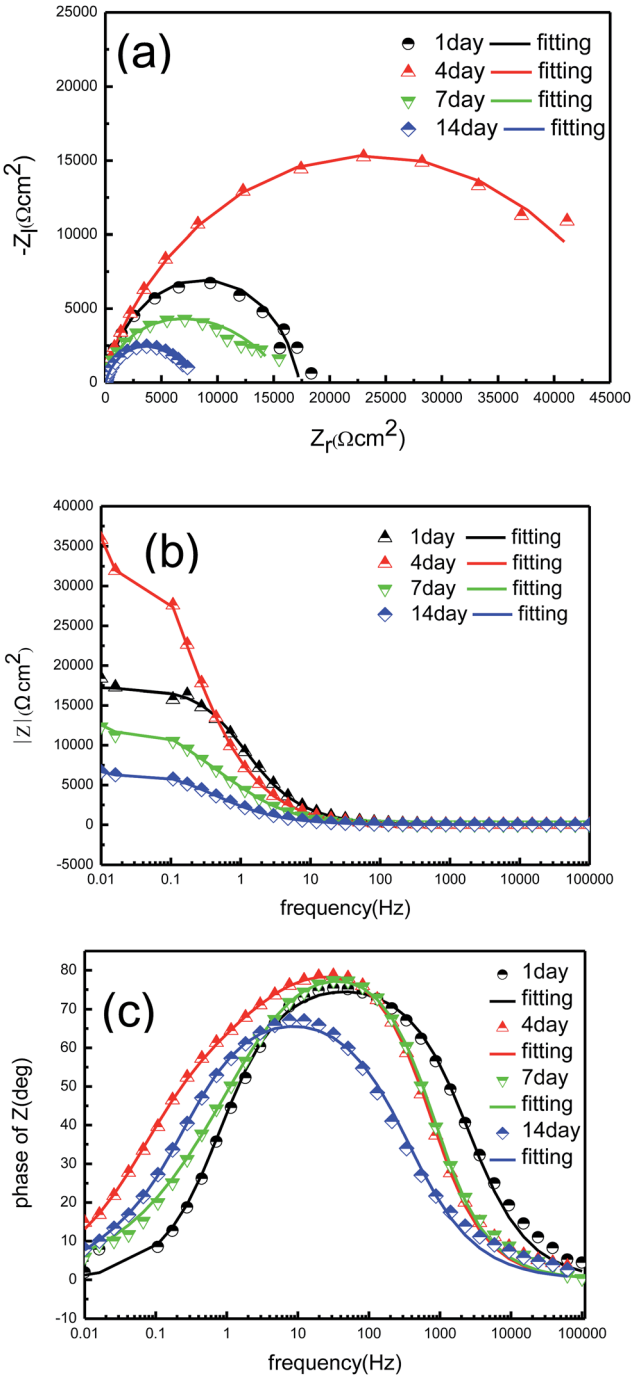

Fig. 8 EIS of the tin-coated copper immersed for different times in the culture medium with BS at 37 °C: (a) Nyquist plot, (b) Bode modulus diagram and (c) Bode phase angle diagram.

Table 2 Fitting parameters of the impedance spectra of tin-coated copper in sterile medium

T (day)	R_s	Q_f	N_1	R_f	Q_p	N_2	R_p	Q_{dl}	N_3	R_{ct}	pH
1	17.04	1.635×10^{-5}	0.896	3.008×10^{4}							6.97
4	15.48				1.574×10^{-5}	0.9008	5.145×10^{4}	6.803×10^{5}	0.8331	4.942×10^{4}	6.92
7	16.32				0.000153	0.6923	3.982×10^{4}	1.328×10^{-5}	0.9279	8.32×10^{4}	7.01
14	17.91				0.0001555	0.7592	82.24	1.651×10^{-5}	0.8516	1.579×10^{5}	7.05

the formation of corrosion products and biofilms in microbial corrosion.[27,28] EIS results and the fitting parameters of the impedance spectra of the tin-coated copper under the sterile aqueous environment are shown in Fig. 7 and Table 2. In addition, the EIS results and the fitting parameters of the impedance spectra of the tin-coated copper under the aqueous environment with BS are shown in Fig. 8 and Table 3.

As shown in Fig. 7c and 8c, the Bode plot shows that one time-constant was present when under the sterile aqueous environment with and without BS for 1 day, which fits well with the circuit (a) in Fig. 9. The Bode plot shows that two time-constants were present when under the sterile aqueous environment without BS for 4 days, which is fitted with the equivalent electrical circuit (b) shown in Fig. 9. The physical model (R(QR)(QR)) corresponding to Fig. 9b represents a layer of dense oxide film. As the immersion time increased, the oxide film became denser, hindering the transfer between the surface of the material and the solution. There is a single impedance loop that increased in diameter in Fig. 7a, which is consistent with the increase in the charge transfer resistance (R_{ct}) in Table 2.

The Bode plots of the sample under the aqueous environment with BS for 4 days in Fig. 8c have two time-constants. The corresponding equivalent circuit (R(Q(R(QR)))) in Fig. 9c represents a layer of nonuniform film. The attachment of bacteria on the surface is reversible in the beginning. The single impedance loop increased in diameter from 1 day to 4 days, as shown in Fig. 8c, which shows that these metabolites hinder the corrosion process. More and more bacteria attached onto the surface with time and the biofilm was formed. The diameters of the impedance loops in the Nyquist plots in Fig. 8a decreased within the first 4 days and then markedly increased, indicating that BS accelerates the corrosion process. The reduction in charge transfer resistance (R_{ct}) and the increase in electric

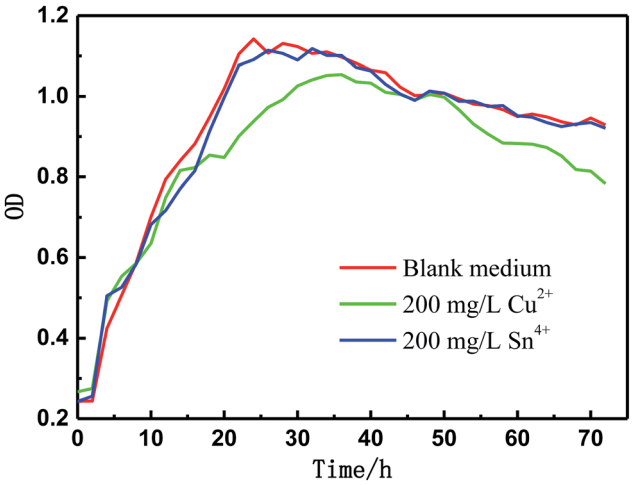

Fig. 10 Growth tendency of BS in sterile culture medium.

Table 3 Fitting parameters of the impedance spectra of tin-coated copper in medium inoculated with *bacteria subtilis*

T (day)	R_s	Q_f	N_1	R_f	Q_b	N_2	R_b	Q_{dl}	N_3	R_{ct}	pH
1	16.68	1.416×10^{-5}	0.8655	1.727×10^{4}							7.01
4	16.62				2.35×10^{-5}	0.9267	7.006×10^{4}	3.306×10^{-5}	0.5958	4.259×10^{4}	8.43
7	15.67				2.27×10^{-5}	0.9284	4247	7.891×10^{-5}	0.5018	1.208×10^{4}	8.73
14	18.73				0.0001197	0.7911	6708	0.003658	0.8257	1134	8.96

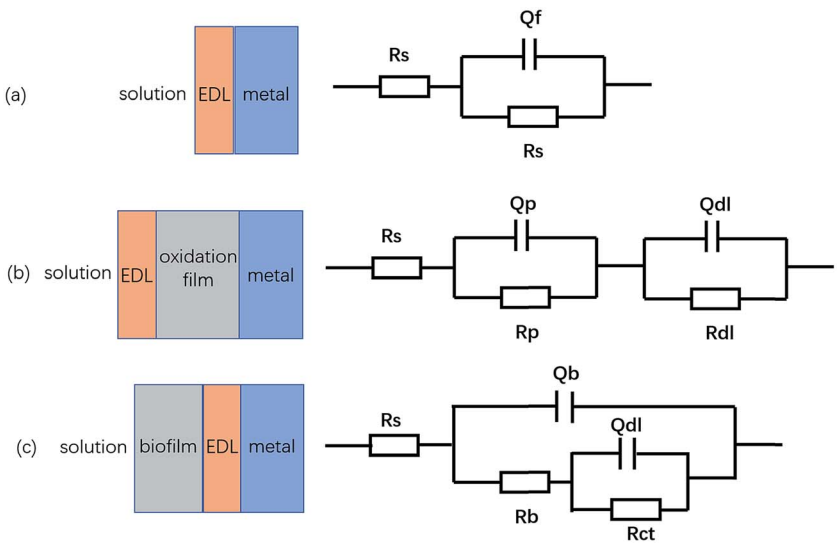

Fig. 9 Physical models and equivalent electrical circuits simulating the EIS diagrams based on (a) a single-layer model, (b) a double-layer model and (c) a double-layer model.

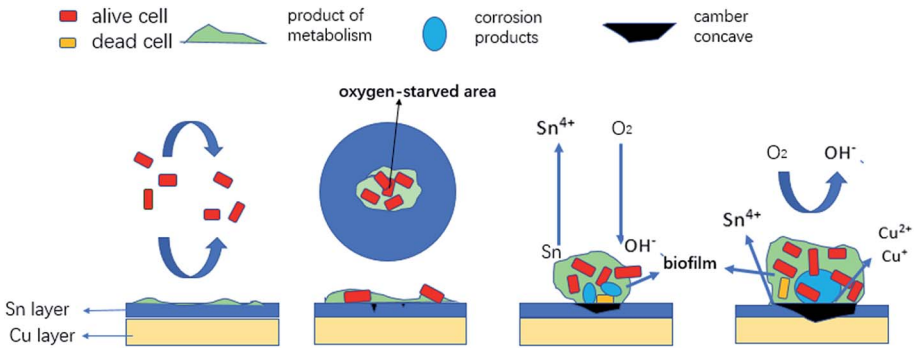

Fig. 11 Schematic diagram for the corrosion process of tin-coated copper in the culture media with *Bacillus subtilis*.

double layer capacitance (Q_{dl}) indicate a decrease in resistance, which can be seen in Table 3. R_{ct} is indicative of the magnitude of the interface reaction resistance and is commonly used to characterise the rate of corrosion. The charge transfer resistance (R_{ct}) was less for the sample under the aqueous environment with BS than that in the sterile environment, indicating that the sample under the aqueous environment with BS was more susceptible to corrosion.

3.5 Mechanism

Oxygen under the aqueous environment without BS loses electrons to produce hydroxide ions, and tin loses electrons to produce tin ions. The hydroxide ions and the tin ions react and form a tin oxide layer, which is insoluble in water. The tin oxide layer hinders the transfer between the solution and sample, which results in the inhibition of the corrosion reaction.

$$O_2 + 2H_2O + 4e^- \rightarrow 4OH^- \quad (1)$$

$$Sn - 2e^- \rightarrow Sn^{2+} \quad (2)$$

$$Sn^{2+} + 2OH^- \rightarrow Sn(OH)_2 \quad (3)$$

$$Sn(OH)_2 + 2OH^- - 2e^- \rightarrow SnO_2 + 2H_2O \quad (4)$$

The corrosion process of the tin-coated copper has four stages, which are shown in Fig. 11. The bacteria are reversibly adsorbed on the surface in the beginning, while some metabolites are adsorbed on the metal surface, which inhibits corrosion. In the second stage, the metabolites are suitable for the bacteria due to their hydrophilicity. In the meantime, the tin ions on the metal surface do not affect the metabolism of the bacteria, which can be seen from the growth tendency of BS under the aqueous environment after adding 200 mg L^{-1} of tin ions (Fig. 10). Lots of bacteria accumulate on the surface and the metabolism of bacteria causes a difference in the oxygen concentration in this area with time. Prior corrosion occurs in the area that is starved of oxygen. In the third stage, more bacteria accumulate on the surface, which consume more oxygen and accelerate the corrosion process.

$$O_2 + 2H_2O + 4e^- \rightarrow 4OH^- \quad (5)$$

$$2Cu - 2e^- \rightarrow 2Cu^+ \quad (6)$$

$$4Cu^+ + 2OH^- \rightarrow Cu_2O + H_2O \quad (7)$$

$$Cu_2O - 2e^- + 2OH^- \rightarrow 2CuO + H_2O \quad (8)$$

Corrosion products in the culture media with BS included Cu(I), Cu(II) and SnO_2. The copper was not completely oxidised, which is probably due to the presence of copper ions. Copper ions have a certain inhibitory effect on bacteria, which can be seen in Fig. 10. The pH of the BS aqueous solution increased from 7.01 to 8.96 with immersion time, indicating that the microbial acid production mechanism is not the main reason for the dissolution of the tin layer in the corrosion process. Differences in oxygen concentration are the main reason for corrosion. Another factor is the formation of the non-uniform biofilm layer, which contains aerobic bacteria, leading to different oxygen concentrations. Another factor is that the biofilm acts as a barrier, preventing the diffusion of oxygen to the metal surface.

4. Conclusion

This study focused on the corrosion behaviour of tin-coated copper caused by BS biofilms. The field emission and XPS data indicated that the tin layer of the sample, which can improve the conductivity and welding properties of copper, was not complete anymore. The FM and the SEM images showed that the BS adhered to the surface and aggregated into an agglomeration. The EIS results show that the metabolites inhibited the corrosion process in the initial stage, while the respiration of BS accelerated the corrosion process and the oxygen-starved zone prior to corrosion. This study removed the possible influence of acid production corrosion and the chloride corrosion. Meanwhile, the effect of bacterial respiration on the metal was revealed, especially when the biofilm was considered to have the ability to hinder the corrosion process. However, the mechanisms behind the effects of the bacterial metabolites on the sample are still unclear. Further study is required to investigate the composition of bacterial metabolites and the role of the composition.

Conflicts of interest

There are no conflicts to declare.

Acknowledgements

This work was supported by the National Natural Science Foundation of China (No. 51671027 & 51271032 & 51131005); National Basic Research Program of China (973 Program) (No. 2014CB643300); and the National Environmental Corrosion Platform (NECP).

References

1 C. D. S. Tuck, C. A. Powell, J. Nuttall and J. A. R. Tony, *Shreirs Corrosion*, Oxford, 2010, pp. 1937–1973.
2 H. Nady, M. El-Rabiei and M. Samy, *Egypt. J. Pet.*, 2016, 26.
3 P. Yi, K. Xiao and K. Ding, *Electron. Mater. Lett.*, 2016, **12**, 163–170.
4 D. Saha, A. Pandya and J. K. Singh, *Atmos. Pollut. Res.*, 2016, **7**, 1037–1042.
5 P. Yi, C. F. Dong and K. Xiao, *Appl. Surf. Sci.*, 2017, **399**, 608–616.
6 K. W. Yee Dennis, *Circuitree*, 2007, **1**, P10.
7 I. B. Beech, *Int. Biodeterior. Biodegrad.*, 2004, **53**, 177–183.
8 D. J. Beale, M. S. Dunn and P. D. Morrison, *Corros. Sci.*, 2012, **55**, 272–279.
9 V. P. Utgikar, H. H. Tabak and and J. R. Haines, *Biotechnol. Bioeng.*, 2003, **82**, 306–312.
10 F. M. Fuchs, A. Driks and P. Setlow, *J. Microbiol. Methods*, 2017, **134**, 7–13.
11 G. O. Oyetibo, M. F. Chien and W. Ikeda-Ohtsubo, *Biodeterior. Biodegrad.*, 2017, **120**, 143–151.
12 T. M. Roane, K. L. Josephson and I. L. Pepper, *Appl. Environ. Microbiol.*, 2001, **67**, 3208–3215.
13 G. O. Oyetibo, M. F. Chien and W. Ikeda-Ohtsubo, *Int. Biodeterior. Biodegrad.*, 2017, **120**, 143–151.
14 L. H. Chen, R. Han, H. Zhang, *et al.*, *Appl. Soil. Ecol.*, 2017, **113**, 127–134.
15 Y. Hong, H. Yongqing and Z. Lantao, *Manned Space Flight*, 2013, **19**, 38–46.
16 L. Fei, Y. Hui and Z. Hui, *Manned Space Flight*, 2014, **5**, 465–473.
17 B. Fanlu, W. Chuanfeng and Z. Lantao, *Life Science Instruments*, 2015, **3**, 16–22.
18 F. J. Passman, *Int. Biodeterior. Biodegrad.*, 2013, **81**, 88–104.
19 B. Palaniappan and S. R. Toleti, *J. Biosci. Bioeng.*, 2015, **121**, 435–441.
20 A. Harimawan, S. Zhong and C. T. Lim, *J. Colloid Interface Sci.*, 2013, **405**, 233–241.
21 S. Liu, H. Dai and C. Heering, *Tetrahedron Lett.*, 2017, **58**, 257–261.
22 R. Zuo, E. Kus and F. Mansfeld, *Corros. Sci.*, 2005, **47**, 279–287.
23 Q. Qu, H. Yue and W. Lei, *Corros. Sci.*, 2015, **91**, 321–329.
24 A. Jayaraman, E. T. Cheng and J. C. Earthman, *Appl. Microbiol. Biotechnol.*, 1997, **48**, 11.
25 A. Jayaraman, E. T. Cheng and J. C. Earthman, *J. Ind. Microbiol. Biotechnol.*, 1997, **18**, 396.
26 M. A. Javed, P. R. Stoddart and E. A. Palombo, *Corros. Sci.*, 2014, **86**, 149–158.
27 D. Zhang, H. Qian, L. Wang and X. Li, *Corros. Sci.*, 2016, **103**, 230–241.
28 D. Xu, J. Xia, E. Zhou, D. Zhang, H. Li, C. Yang, Q. Li, H. Lin, X. Li and K. Yang, *Bioelectrochem*, 2017, **113**, 1–8.